# Synthesis, Characterization, and Properties Evaluation of Methylcoumarin End-Functionalized Poly(methyl methacrylate) for Photoinduced Drug Release

**Carsten Sinkel, Andreas Greiner, and Seema Agarwal***

*Philipps-Universität Marburg, Fachbereich Chemie, und Wissenschaftliches Zentrum für Materialwissenschaften, Hans-Meerwein Strasse, D-35032, Marburg, Germany*

*Received November 26, 2007; Revised Manuscript Received February 5, 2008*

ABSTRACT: The synthesis of novel methylcoumarin end-functionalized poly(methyl methacrylate) of different molecular weights using atom transfer radical polymerization (ATRP) is reported. 7-(2′-Bromoisobutyryloxy)-4-methylcoumarin was used as the ATRP initiator at 70 °C using copper(I) bromide/1,1,4,7,7-pentamethyldiethylenetriamine (PMDETA) as the catalyst system. The theoretical and experimental number-average molecular weights $M_n$ with narrow polydispersities ($M_w/M_n = 1.1-1.4$) agreed very well. Photochemical drug loading of the methylcoumarin end-functionalized polymer was performed in solution (chloroform/acetone 1:2) with benzophenone as additional photosensitizer using a 50-fold excess of the pro-drug 1-heptanoyl-5-fluorouracil (H5FU). UV/vis and NMR spectroscopy were used for the characterization of the polymer drug conjugate and indicated an almost quantitative conversion of coumarin moieties into photodimers. The change of polymer properties like thermal stability, glass transition, and molecular weight after photochemical drug immobilization was also studied. The glass transition temperature increased only negligibly, whereas the thermal decomposition commenced at considerably lower temperature for the polymer drug conjugate. The molecular weight distribution of the H5FU-loaded polymer showed no detectable chain degradation due to the applied UV irradiation. The characterization of the photoinduced drug release was investigated for a single photon absorption (SPA) process. The polymer drug conjugate was irradiated at $\lambda = 266$ nm to cleave the cyclobutane linker between the methylcoumarin moiety and the pro-drug H5FU. The drug release was monitored and quantified using high-performance liquid chromatography (HPLC). Assuming quantitative hydrolysis of H5FU, 4.76 $\mu$g of 5-fluorouracil (5FU) per 1 mg of polymer drug conjugate was released on irradiation.

## Introduction

The development of new polymer-based technologies for controlled drug release is among the fastest evolving research areas in medicinal chemistry.[1] The advantages of such polymer-based systems are numerous and include improved efficacy, reduced toxicity, and improved patient compliance and convenience compared to conventional drug administration forms. In principle, there are two types of control over drug release that can be realized—distributional and temporal control.[1] A distributional control is especially beneficial if uniform drug distribution damages healthy tissue, which is often the case for chemotherapeutics or if the drug is prevented (e.g., by the blood−brain barrier) from reaching its molecular site of action.[2] For most diseases that require a distribution controlled release of drug, a targeting mechanism must be designed that allows the delivery system to find the desired target.[3] The easiest way to ensure a spatially confined drug distribution is to implant the drug delivery system directly at the site as described by Brem et al. for the chemotherapeutic treatment of malignant gliomas after surgical removal of the tumor.[4]

Polymeric systems for temporally controlled drug delivery provide sustained release by mechanisms such as delayed dissolution of drug molecules, inhibited drug diffusion from the depot, or controlled flow of drug solution.[5] In contrast to sustained release systems, which start to deliver the drug as soon as they are applied to the patient, responsive drug delivery devices release the drug in a pulsating manner and only if stimulated by the change of an environmental parameter or by an external impulse. Such parameters include pH or temperature changes as well as magnetic, electric, or ultrasonic impulses.[6] We are particularly interested in photoinduced drug release from implanted intraocular lenses (IOLs) used in cataract surgery.

A cataract is an opacity developing in the crystalline lens of the human eye and if untreated may cause irreversible loss of vision. The major postoperative complication is posterior capsule opacification (PCO), the so-called secondary cataract. A proliferation and migration of lens epithelial cells into the visual axis lead to a new deterioration of vision. The conventional and currently only effective treatment of PCO is Nd:YAG laser capsulotomy, during which a high-energy laser beam disrupts the opacified tissue membrane. However, this treatment sometimes leads to serious complications, including alterations of the IOL optic,[7,8] increased intraocular pressure,[9,10] or retinal detachment.[11,12]

Recently, we and others reported a novel photoresponsive drug delivery system for intraocular lenses used in cataract surgery equipped with a multidose drug depot.[13–16] The cell toxic pro-drug 1-heptanoyl-5-fluorouracil (H5FU) was immobilized on a coumarin multifunctionalized acrylic copolymer via a polymer analogous photochemical reaction (photoreversible [2 + 2]-cycloaddition). The major drawback of this approach is the high degree of mainly intramolecular cross-linking during photochemistry and therefore a decline in the mechanical properties, polymer processability, and transparency of lens precursors.

Here we report the synthesis of a novel methylcoumarin end-functionalized acrylic polymer by atom transfer radical polymerization (ATRP). The use of 7-(2′-bromoisobutyryloxy)-4-methylcoumarin as ATRP initiator led to the polymer chain end functionalization with methylcoumarin moieties. To circumvent the inherent cross-linking reactions during polymer analogous photochemistry, the amount of photoreactive linker groups was reduced to one moiety per polymer chain. To achieve the

* Correponding author. E-mail: seema@chemie.uni-marburg.de.

10.1021/ma702622p CCC: $40.75 
Published on Web 04/30/2008

**Scheme 1. Synthesis of a Polymer Drug Conjugate C for Photoinduced Release**[a]

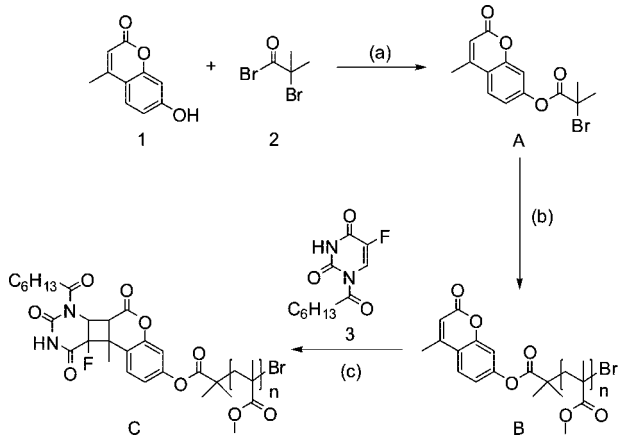


[a] Conditions: (a) $NEt_3$, dichloromethane, 0°C; (b) methyl methacrylate, Cu(I)Br/1,1,4,7,7-pentamethyldiethylenetriamine, anisole, 70 °C; (c) benzophenone, chloroform/acetone (1:2), UVA irradiation ($\lambda_{max}$ = 350 nm).

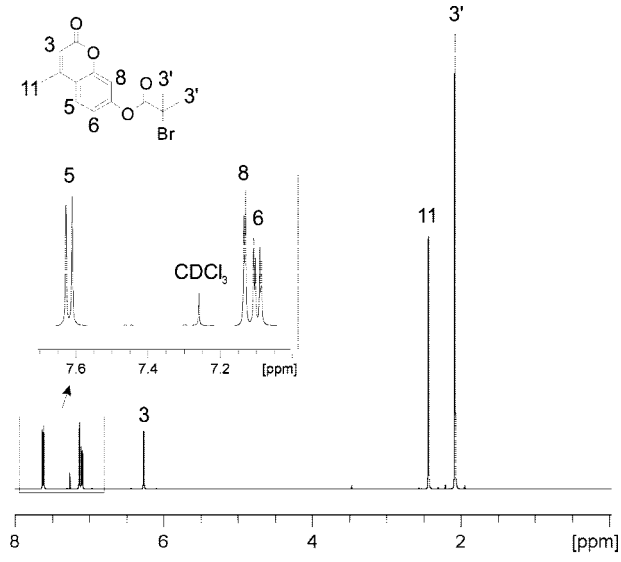


**Figure 1.** $^1$H NMR (500.13 MHz, $CDCl_3$) spectrum of 7-(2′-bromoisobutyryloxy)-4-methylcoumarin, **A**.

necessary immobilized pro-drug concentration in the final polymeric lens precursor, short functionalized polymer chains were essential. The chain length control was achieved using the ATRP technique. The first results of this novel approach are discussed in detail in this work.

## Experimental Section

**Materials.** Methyl methacrylate (MMA, BASF, 99%), triethylamine (BASF, 99.7%), and anisole (Acros, 99%) were dried over calcium hydride, distilled, and stored under argon. Acetone (BASF) was purified by distillation over potassium carbonate. Chloroform (BASF) was purified by distillation over calcium chloride. Dichloromethane (DCM, BASF), ethanol (BASF), tetrahydrofuran (THF, BASF), and hexane (BASF) were purified by distillation. Acetonitrile (HPLC grade, Acros), Cu(I)Br (Aldrich, 99.999%), 1,1,4,7,7-pentamethyldiethylenetriamine (PMDETA, Acros, 99+%), 2-bromoisobutyryl bromide (Aldrich, 98%), 7-hydroxy-4-methylcoumarin (Acros, 97%), and 5-fluorouracil (5FU, Alfa Aesar, 99%) were used as received. Benzophenone (BASF) was recrystallized from ethanol. 1-Heptanoyl-5-fluorouracil (H5FU) was synthesized starting with 5-fluorouracil (5FU) according to a literature procedure.[14,17]

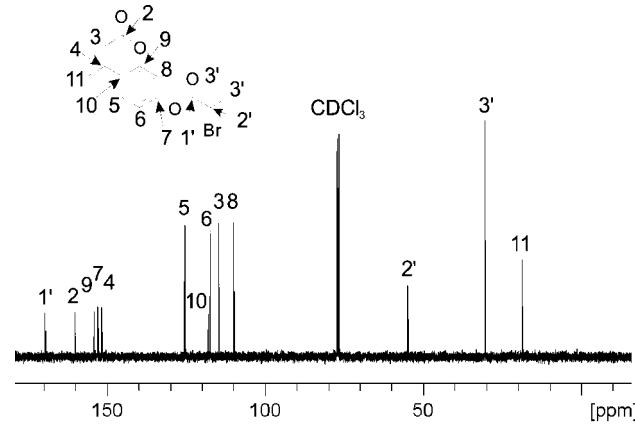


**Figure 2.** $^{13}$C NMR (125.77 MHz, $CDCl_3$) spectrum of 7-(2′-bromoisobutyryloxy)-4-methylcoumarin, **A**.

**Instrumentation.** The number-average molecular weights ($M_n$) and the weight-average molecular weights ($M_w$) of the polymers were determined by gel permeation chromatography (GPC) using a Knauer system equipped with a PSS-SDV (10 $\mu$m) 50 × 8 mm$^2$ column and two columns 600 × 8 mm$^2$ at 25 °C, a differential refractive index detector, and a UV photometer using THF as eluent at a flow rate of 0.8 mL/min. Poly(methyl methacrylate) (PMMA) standards were used for calibration.

$^1$H (300.13 MHz) and $^{13}$C (75.47 MHz) NMR spectra were recorded on Bruker Avance 300 A and Avance 300 B spectrometers, respectively, using $CDCl_3$ as solvent. $^1$H (500.13 MHz) and $^{13}$C (125.77 MHz) NMR spectra were recorded on a Bruker Avance DRX-500 spectrometer using $CDCl_3$ as solvent. $^{19}$F (282.40 MHz) NMR spectra were recorded on a Bruker Avance 300 A spectrometer. $^1$H−$^{13}$C correlation experiments were performed on a Bruker DRX-500 spectrometer, with a 5 mm multinuclear gradient probe and using gs-HMQC (heteronuclear multiple quantum correlation) and gs-HMBC (heteronuclear multiple bond correlation) pulse sequences. The HMQC experiment was optimized for C−H coupling of 140 Hz, with decoupling applied during acquisition, while the HMBC experiment was optimized for coupling of 8 Hz, with decoupling during acquisition. 2D NMR data were acquired with 2048 points in $t_2$, and the number of increments for $t_1$ was 256. Four and eight scans were used for HMQC and HMBC experiments, respectively, and dummy scans of four were used for both experiments. A relaxation delay of 1 s was used for all 1D experiments and 2 s for all 2D experiments. A typical experiment time was about 1.5 and 3.0 h for HMQC and HMBC, respectively.

Mettler thermal analyzers having 851 TG and 821 DSC modules were utilized for the thermal characterization of the polymers. Indium and zinc standards were used for temperature and enthalpy calibration of the 821 DSC module. Differential scanning calorimetric (DSC) scans were recorded in nitrogen atmosphere (flow rate = 80 mL/min) at a heating rate of 10 °C/min. The melting temperatures ($T_m$) were determined from the endothermic peak maximum of the first heating cycle. The glass transition temperature ($T_g$) was taken as the inflection point of the observed shift in the baseline of the second heating cycle of a DSC scan. Thermal stability was determined by recording thermogravimetric (TG) traces in nitrogen atmosphere (flow rate = 50 mL/min) using powdered samples. A heating rate of 10 °C/min and a sample size of 10 ± 2 mg were used in each experiment.

Polymer analogue photodimerization reactions were performed in a Rayonet-type photoreactor equipped with 12 concentrically arranged UV-light tubes (Eversun L 40W/79) and a rotating sample holder to ensure uniform irradiation. Drug release by single photon absorption (SPA) was carried out using a Shimadzu spectrofluorometer model RF-1502 at $\lambda$ = 266 nm. All samples were dissolved in THF, transferred into a 10 mm path length quartz cuvette, and stirred during irradiation.

High-performance liquid chromatographic (HPLC) analysis was carried out using a Hewlett-Packard model 1090 system with diode

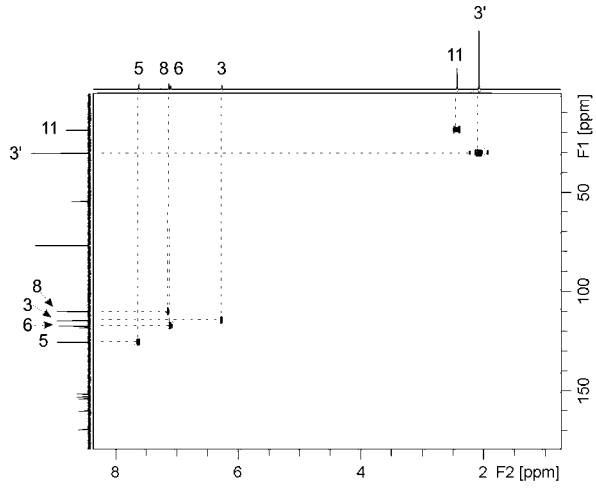


**Figure 3.** 2D $^{1}H-^{13}C$ correlation NMR experiment (heteronuclear multiple quantum coherence HMQC) of 7-(2′-bromoisobutyryloxy)-4-methylcoumarin, **A**.

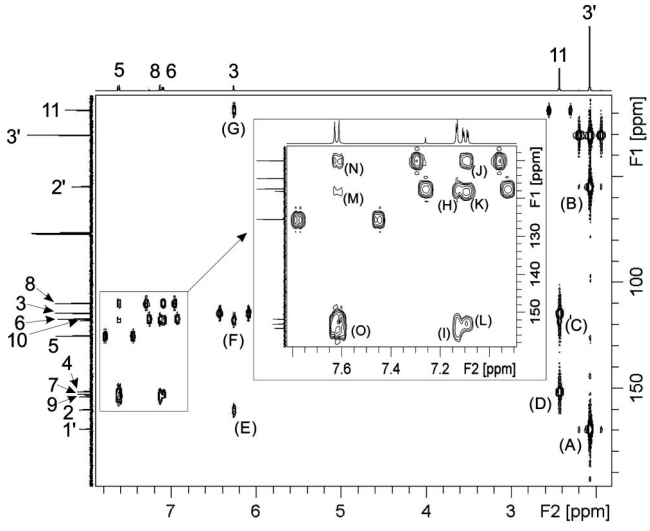


**Figure 4.** $^{1}H-^{13}C$ correlation NMR experiment (heteronuclear multiple bond correlation HMBC) of 7-(2′-bromoisobutyryloxy)-4-methylcoumarin, **A**.

array detector model 1040 (266 nm trace was used for quantification) equipped with a RP-18 column (LiChrospher 100RP18-5$\mu$m). Applied isocratic method: acetonitrile/water (50:50 v/v), column temperature = 40 °C, flow rate = 1 mL/min. The injection volume was 20 $\mu$L. For quantitative determination of 5-fluorouracil (5FU) and 1-heptanoyl-5-fluorouracil (H5FU) calibration sequences were measured using 5FU and H5FU standards (0.045−2 mmol/L), respectively, in THF.

FTIR spectra were recorded on a Digilab Excalibur system using a Pike Miracle attenuated total reflection (ATR) unit.

A Perkin-Elmer Lambda 9 UV/vis/NIR spectrophotometer was used for UV/vis absorption spectroscopy.

Gas chromatographic (GC) analysis was carried out using a Shimadzu GC-17A system with flame ionization detector (FID). Injector and detector temperatures were set to 300 °C. Applied temperature profile modified for detection of MMA and anisole in *n*-hexane solution: 5 min 30 °C, 11 min 60 °C (5 °C/min), 12 min 60 °C, 16 min 80 °C (5 °C/min). A standard calibration curve of MMA in anisole was used for following the reaction kinetics.

Elemental analysis was carried out on a Hereaus CHN-Rapid machine.

**Synthesis of 7-(2′-Bromoisobutyryloxy)-4-methylcoumarin (A).** A dry two-necked round-bottom flask was charged with a suspension of 7-hydroxy-4-methylcoumarin, **1** (20.0 g, 114 mmol), in dichloromethane (200 mL). Triethylamine (11.6 g, 115 mmol, 1 equiv) was added, and the reaction mixture was cooled to 0 °C and stirred for 30 min before 2-bromoisobutyryl bromide **2** (31.6 g, 138 mmol, 1.2 equiv) was added dropwise. After reaction for 2 h at 0 °C, complete conversion of **1** was achieved. The precipitated ammonium salt was filtered off and washed with dichloromethane. The pale yellow filtrate was washed twice with dilute hydrochloric acid and water. The organic layer was dried over sodium sulfate, and the solvent was subsequently removed under reduced pressure. The pale yellow solid was purified by recrystallization from methanol (400 mL) to yield product **A** as colorless needles. Yield: 27.1 g (73%). $T_m$ = 123 °C (DSC). $^{1}H$ NMR (500.13 MHz, $CDCl_3$), $\delta$/ppm: 7.62 (d, $J$ = 8.6 Hz, 1 H, C5H), 7.13 (d, $J$ = 2.3 Hz, 1 H, C8H), 7.1 (dd, $J$ = 8.6, 2.3 Hz, 1 H, C6H), 6.27 (d, $J$ = 1.1 Hz, 1 H, C3H), 2.43 (d, $J$ = 1.2 Hz, 3 H, C11$H_3$), 2.07 (s, 6 H, 2 × C3′$H_3$). $^{13}C$ NMR (125.77 MHz, $CDCl_3$), $\delta$/ppm: 169.6 (C1′), 160.2 (C2), 154.2 (C9), 153.0 (C7), 151.8 (C4), 125.5 (C5), 118.1 (C10), 117.4 (C6), 114.7 (C3), 110.0 (C8), 54.9 (C2′), 30.4 (C3′), 18.7 (C11). FTIR (ATR), $\nu$/cm$^{-1}$: 3094 $\nu$($C_{sp^2}$−H), 3071 $\nu$($C_{sp^2}$−H), 3006 $\nu$($C_{sp^2}$−H), 2985 $\nu$($C_{sp^3}$−H), 2935 $\nu$($C_{sp^3}$−H), 1757 $\nu$(C═O), 1708 $\nu$(C═O), 1613 $\nu$(C═C), 1572 $\nu$(C═C), $\nu$(C−O), 1135 $\nu$(C−O), 1095 $\nu$(C−O). Anal. Calcd for $C_{14}H_{13}BrO_4$: C, 51.71%; H, 4.03%; Br, 24.57%. Found: C, 51.82%; H, 4.07%; Br, 23.86%.

**General Procedure for Polymerization in Solution.** A dry Schlenk tube equipped with a magnetic stir bar was charged with copper(I) bromide (61.2 mg, 0.43 mmol, 0.25 equiv) and **A** (555 mg, 1.71 mmol, 1 equiv). The flask was sealed with a rubber septum and cycled between vacuum and argon twice to remove oxygen. Anisole (20 mL), methyl methacrylate (20.0 mL, 188 mmol, 110 equiv), and 1,1,4,7,7-pentamethyldiethylenetriamine (89 $\mu$L, 0.43 mmol, 0.25 equiv) were added using argon flushed syringes. Subsequently, three freeze−pump−thaw cycles were performed, and the tubes were immersed in an oil bath at 70 °C. After 18 h, the polymerization was stopped by cooling the Schlenk tubes in liquid nitrogen. The reaction mixture was then diluted with an equal amount of dichloromethane. Subsequently, the copper catalyst was removed using a short alumina column. After concentration of the purified solution, the methylcoumarin end-functionalized polymer **B** was precipitated from ethanol and collected by filtration. Conversion: 62%. $M_n$ = 6020, $M_w/M_n$ = 1.15. $T_g$ = 115 °C. $T_{5\%}$ = 371 °C. $^{1}H$ NMR (300.13 MHz, $CDCl_3$), $\delta$/ppm: 7.57 (d, $J$ = 8.6 Hz, 1 H, C5H), 7.05−6.95 (m, 2 H, C6H, C8H), 6.23 (s, 1 H, C3H), 3.55 (bs, 221 H, −$OCH_3$), 2.4 (s, 3 H, C11$H_3$), 2.1−0.7 (m, 377 H, polymer backbone).

**Polymerization Kinetics.** The following procedure was used for polymerization kinetic studies. A dry Schlenk tube equipped with a magnetic stir bar was charged with copper(I) bromide (168 mg, 1.17 mmol, 0.25 equiv) and **A** (1.528 g, 4.7 mmol, 1 equiv). The flask was sealed with a rubber septum and cycled between vacuum and argon twice to remove oxygen. Anisole (25 mL), methyl methacrylate (25.0 mL, 235 mmol, 50 equiv), and 1,1,4,7,7-pentamethyldiethylenetriamine (245 $\mu$L, 1.17 mmol, 0.25 equiv) were added using argon-flushed syringes. Subsequently, three freeze−pump−thaw cycles were performed, and the tubes were immersed in an oil bath at 70 °C. At timed intervals samples were withdrawn using argon-flushed syringes and added to an equal amount of cold THF to stop further polymerization. The copper catalyst was removed using short alumina columns. Subsequently, the polymer solution was concentrated, and the polymer was precipitated from *n*-hexane. To determine the extent of conversion, a 100 $\mu$L sample of the THF-diluted reaction mixture was added to 10 mL of *n*-hexane, the polymer was filtered off, and the solution was used for GC analysis with anisole as internal standard.

**Photochemical Drug Loading.** A dry round-bottom flask was charged with methylcoumarin end-functionalized polymer **B** ($M_n$ = 6020) (2.0 g), 1-heptanoyl-5-fluorouracil, **3** (3.19 g, 13.2 mmol, 50 equiv calculated to amount of coumarin units), and benzophenone (48.5 mg, 2.66 mmol, 1 equiv). Acetone (100 mL) and chloroform (50 mL) were added. Argon was bubbled through the colorless solution for half an hour to remove oxygen. Subsequently, the reaction mixture was distributed to 10 sealable reaction tubes

**Table 1. Experimental Details and Analytic Data of Methyl Methacrylate (MMA) Atom Transfer Radical Polymerizations Initiated by 7-(2′-Bromoisobutyryloxy)-4-methylcoumarin, A[a]**

| | molar feed ratio | | | | | | | |
|---|---|---|---|---|---|---|---|---|
| no. | MMA | **A** | catalyst | conversion/% | $M_n \times 10^{-3}$ (NMR)[b] | $M_n \times 10^{-3}$ (GPC)[c] | $M_w/M_n$[d] | $M_{n,theor} \times 10^{-3}$ [e] |
| 1 | 100 | 1 | 1 | 92 | 14.5 | 16.6 | 1.38 | 9.5 |
| 2 | 100 | 1 | 0.5 | 64 | 11.1 | 10.6 | 1.26 | 6.7 |
| 3 | 100 | 1 | 0.25 | 60 | 7.9 | 8.0 | 1.13 | 6.3 |
| 4 | 50 | 1 | 0.25 | 85 | 4.8 | 4.3 | 1.24 | 4.6 |
| 5 | 25 | 1 | 0.25 | 81 | 2.5 | 3.1 | 1.32 | 2.4 |
| 6 | 10 | 1 | 0.25 | 85 | 1.8 | 1.5 | 1.24 | 1.2 |

[a] Catalyst: Cu(I)Br/1,1,4,7,7-pentamethyldiethylenetriamine (1:1, molar ratio), reaction time = 4 h, $[MMA]_0 = 4.69$ M (anisole solution), reaction temperature = 70 °C. [b] Number-average molecular weight ($M_n$) calculated by $^1$H NMR spectroscopy from the resonances of the methyl ester groups of poly(methyl methacrylate) between 3.51 and 3.58 ppm and the C5H aromatic proton of the coumarin functionality at 7.6 ppm (refer to Figure 5). [c] Number-average molecular weight ($M_n$) determined by GPC (gel permeation chromatography). [d] Polydispersity ($M_w/M_n$); $M_w$ (weight-average molecular weight) and $M_n$ were determined by GPC. [e] $M_{n,theor}$ = molar mass **A** + conversion/100 × molar mass MMA × [MMA]/[**A**].

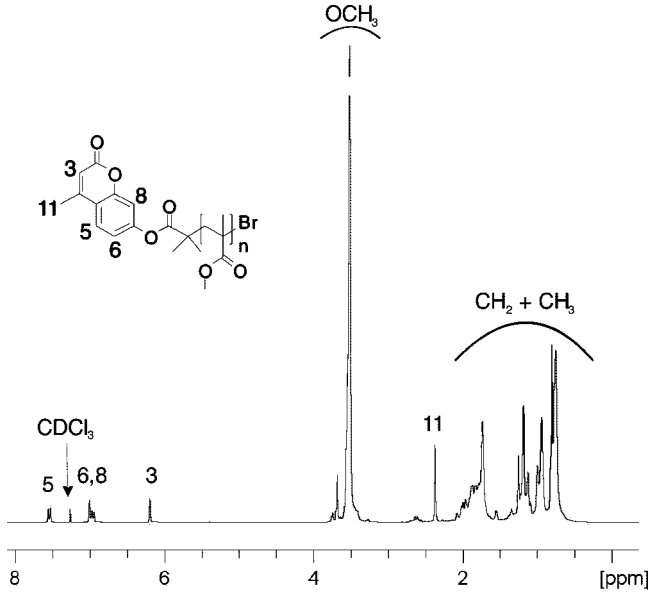


**Figure 5.** $^1$H NMR (300.13 MHz, $CDCl_3$) spectrum of methylcoumarin end-functionalized poly(methyl methacrylate) **B** (number-average molecular weight $M_n$ = 1500). For experimental details, see no. 6 in Table 1.

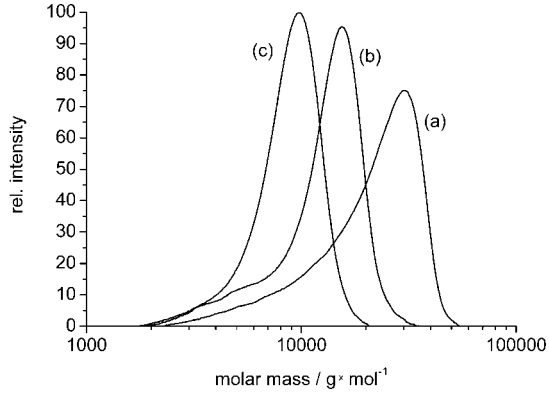


**Figure 6.** Gel permeation chromatographic profiles of methyl methacrylate atom transfer radical polymerizations initiated by 7-(2′-bromoisobutyryloxy)-4-methylcoumarin, **A**. For experimental details see Table 1: (a) run no. 1, (b) run no. 2, and (c) run no. 3.

equipped with a magnetic stir bar, each containing 15 mL. These tubes were sealed under argon, placed in a rotating sample holder to ensure uniform irradiation, and irradiated for 20 h in a Rayonet-type photoreactor with broadband UVA light ($\lambda_{max}$ = 350 nm). The resulting yellow solutions were combined, and the mixture was concentrated under reduced pressure. The polymer was precipitated from 400 mL of ethanol. For further purification the polymer drug conjugate **C** was redissolved in DCM and precipitated again from

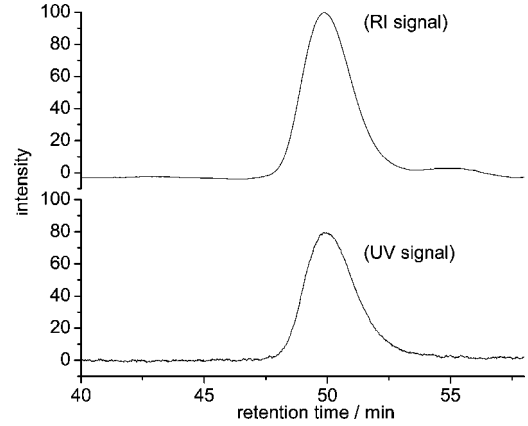


**Figure 7.** Comparison of gel permeation chromatograms recorded with RI and UV detectors for methylcoumarin end-functionalized poly(methyl methacrylate) **B**. [Methyl methacrylate, $MMA]_0$ = 4.69 M (anisole solution), [7-(2′-bromoisobutyryloxy)-4-methylcoumarin, **A**$]_0$ = 42.6 mM, $[Cu(I)Br]_0$ = [1,1,4,7,7-pentamethyldiethylenetriamine, PMDETA$]_0$ = 10.7 mM, (MMA:**A**:CuBr:PMDETA = 110:1:0.25:0.25, molar ratio); reaction temperature = 70 °C; reaction time = 18 h.

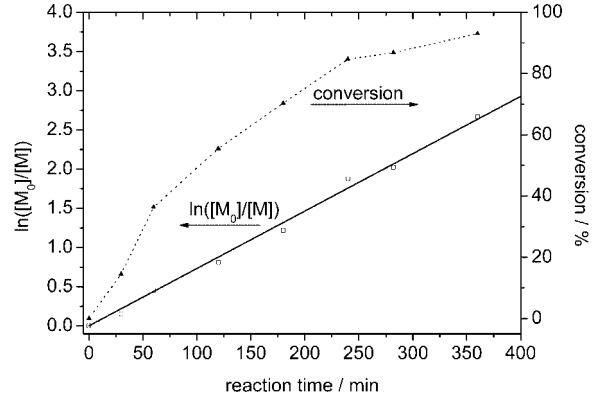


**Figure 8.** Monomer conversion with polymerization time and kinetic plot for methyl methacrylate polymerization under atom transfer radical polymerization conditions initiated by 7-(2′-bromoisobutyryloxy)-4-methylcoumarin, **A**. For experimental details see Table 2.

400 mL of ethanol. Yield: 1.09 g. $M_n$ = 7200, $M_w/M_n$ = 1.25. $T_g$ = 121 °C. $T_{5\%}$ = 284 °C. $^1$H NMR (300.13 MHz, $CDCl_3$), $\delta$/ppm: 8.04 (bs, N3H), 6.84−6.76 (m, 3 H, C5H, C6H, C8H), 5.16 (s, cyclobutane proton), 5.09 (s, cyclobutane proton), 3.54 (bs, 285 H, $-OCH_3$), 2.1 − 0.5 (m, 506 H). $^{19}$F NMR (282.40 MHz, $CDCl_3$), $\delta$/ppm: −138.2.

**Drug Release by Single Photon Absorption (SPA).** For HPLC detection and quantification of released pro-drug H5FU, the polymer drug conjugate **C** (8.7 mg) was dissolved in THF (3 mL), transferred into a quartz cuvette equipped with a magnetic stir bar, and irradiated at $\lambda$ = 266 nm for 2.5 h under continuous stirring. After

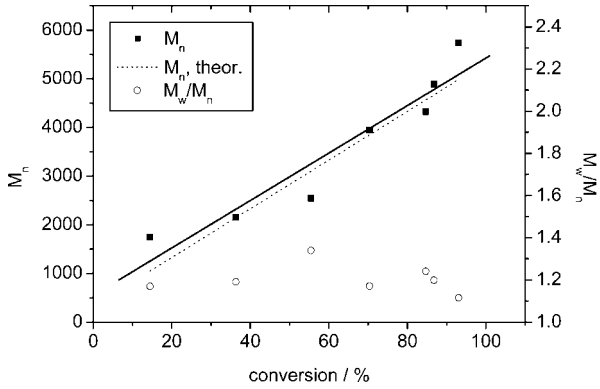


**Figure 9.** Conversion dependence of number-average molecular weight $M_n$ and polydispersity $M_w/M_n$ for methyl methacrylate polymerization under atom transfer radical polymerization conditions initiated by 7-(2′-bromoisobutyryloxy)-4-methylcoumarin, **A**. For experimental details, see Table 2.

**Table 2. Polymerization Kinetics of Methyl Methacrylate (MMA) Atom Transfer Radical Polymerization Initiated by 7-(2′-Bromoisobutyryloxy)-4-methylcoumarin (A)[a]**

| reaction time/min | conversion/% | $M_n \times 10^{-3}$ (GPC)[b] | $M_w/M_n$[c] | $M_{n,theor} \times 10^{-3}$ [d] |
|---|---|---|---|---|
| 30 | 15 | 1.8 | 1.17 | 1.1 |
| 60 | 36 | 2.2 | 1.19 | 2.1 |
| 120 | 56 | 2.6 | 1.34 | 3.1 |
| 180 | 70 | 4.0 | 1.17 | 3.8 |
| 240 | 85 | 4.3 | 1.24 | 4.6 |
| 282 | 87 | 4.9 | 1.20 | 4.7 |
| 360 | 93 | 5.7 | 1.12 | 5.0 |

[a] $[MMA]_0 = 4.69$ M (anisole solution), $[A]_0 = 93.8$ mM, $[Cu(I)Br]_0 = [1,1,4,7,7\text{-pentamethyldiethylenetriamine}]_0 = 23.5$ mM (MMA:**A**:Cu(I)Br:1,1,4,7,7-pentamethyldiethylenetriamine = 50:1:0.25:0.25, molar ratio); reaction temperature = 70 °C. [b] Number-average molecular weight ($M_n$) determined by GPC (gel permeation chromatography). [c] Polydispersity ($M_w/M_n$); $M_w$ (weight-average molecular weight) and $M_n$ were determined by GPC. [d] $M_{n,theor}$ = molar mass **A** + conversion/100 × molar mass MMA × [MMA]/[**A**].

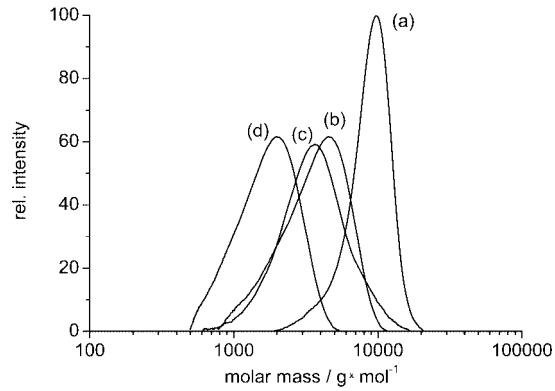


**Figure 10.** Gel permeation chromatographic profiles of methyl methacrylate (MMA) atom transfer radical polymerizations initiated by 7-(2′-bromoisobutyryloxy)-4-methylcoumarin (**A**) in dependence of the MMA/**A** feed ratio. For experimental details, see Table 1: (a) run no. 3, (b) run no. 4, (c) run no. 5, and (d) run no. 6.

given intervals, UV/vis absorption spectra were recorded and 100 μL samples were drawn for HPLC analysis.

## Results and Discussion

**Polymer Synthesis.** 7-(2′-Bromoisobutyryloxy)-4-methylcoumarin (**A**) was synthesized by esterification of 7-hydroxy-4-methylcoumarin (**1**) with 2-bromoisobutyryl bromide (**2**) under basic conditions in dichloromethane at 0 °C, as shown in Scheme 1. The structural characterization was carried out using

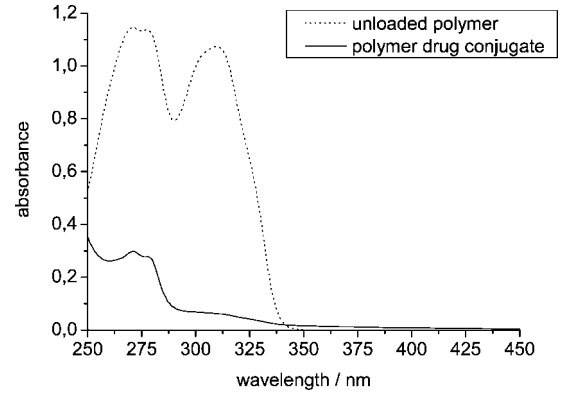


**Figure 11.** UV/vis absorption spectra of methylcoumarin end-functionalized poly(methyl methacrylate) (no. 7, Table 3) prior to and after drug loading process (no. 8, Table 3).

**Table 3. Polymer Properties of Methylcoumarin End-Functionalized Poly(methyl methacrylate) (No. 7) and the Corresponding Polymer Drug Conjugate (No. 8); for Experimental Details See Experimental Section**

| no. | $M_n$[a] | $M_w/M_n$[b] | $T_g$/°C[c] | $T_{5\%}$/°C[d] |
|---|---|---|---|---|
| 7 | 6020 | 1.15 | 115 | 371 |
| 8 | 7200 | 1.25 | 121 | 284 |

[a] Number-average molecular weight ($M_n$) determined by GPC (gel permeation chromatography). [b] Polydispersity ($M_w/M_n$); $M_w$ (weight-average molecular weight) and $M_n$ were determined by GPC. [c] Glass transition temperature ($T_g$). [d] Temperature at which the polymer sample lost 5% of the initial weight as determined by thermogravimetric analysis.

NMR spectroscopic techniques. $^1$H and $^{13}$C NMR spectra are given in Figures 1 and 2. The ratio of resonance integrations in the $^1$H NMR spectrum is in accordance with structure **A**. The $^{13}$C NMR resonances were assigned using correlations observed in the 2D HMQC NMR spectrum (Figure 3). Further confirmation and unambiguous resonance assignments were carried out using the 2D HMBC NMR spectrum in Figure 4. The methyl protons (C3′H$_3$) at 2.07 ppm showed 3 and 2 bond correlations with carbon C1′ (A, 169.6 ppm) and C2′ (B, 54.9 ppm). The methyl protons C11H$_3$ showed characteristic correlations with carbons C3 (C) and C4 (D) at 114.7 and 151.8 ppm, respectively. The 2 and 3 bond correlations of hydrogen C3H were observed as cross-resonances E, F, and G with carbons C2 (160.2 ppm), C10 (118.1 ppm), and C11 (18.7 ppm), respectively. Proton C8H showed correlations with carbon resonances at 117.4 and 118.1 ppm (H) (carbons C6 and C10) and 153.0 and 154.2 ppm (I) (carbons C7 and C9). Proton C6H showed correlation with carbons C8 (J), C10 (K), and C7 (L). The proton resonance at 7.62 ppm (C5H) showed a clear correlation with the carbon C10 at 118.0 ppm (M) besides showing other expected correlations with carbons at 110.0 ppm (N, C8) and at 153.0 and 154.2 ppm (O, C7, and C9). This α-bromoester was subsequently employed as an initiator for the synthesis of methylcoumarin end-functionalized oligo- and poly(methyl methacrylate) (OMMA and PMMA) **B** under ATRP reaction conditions using Cu(I)Br/1,1,4,7,7-pentamethyldiethylenetriamine as the catalyst system. All polymerizations used an equimolar ratio of transition metal to ligand. Different polymerization reactions were carried out in anisole at 70 °C using a 100:1 MMA to initiator molar ratio in order to optimize reaction conditions and varied ratios of initiator to catalyst (Table 1). The obtained polymers were compared for their theoretical molecular weights and the experimentally obtained molecular weights by GPC and by NMR. The representative $^1$H NMR spectrum of PMMA initiated by 7-(2′-bromoisobutyryloxy)-4-methylcoumarin (**A**) is shown in Figure 5. The characteristic aromatic proton resonances of the methylcoumarin functionality are present between 7.0 and 7.6 ppm and are well separated

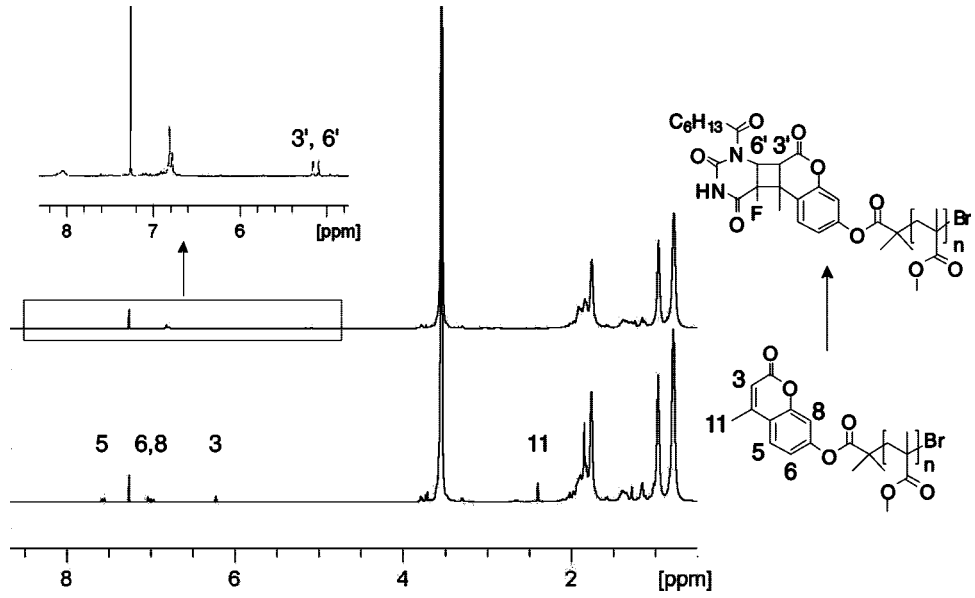


**Figure 12.** $^1$H NMR (300.13 MHz, $CDCl_3$) spectra of methylcoumarin end-functionalized poly(methyl methacrylate) (no. 7, Table 3) and polymer drug conjugate (no. 8, Table 3).

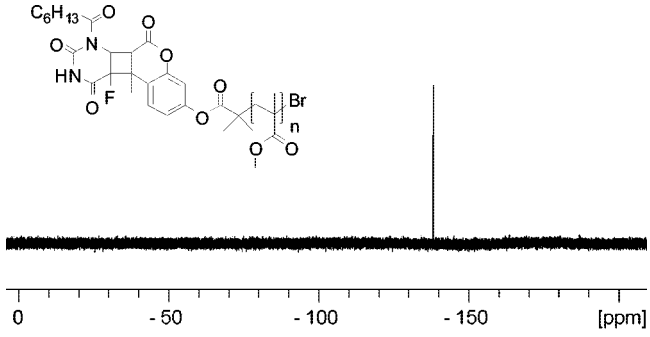


**Figure 13.** $^{19}$F NMR (282.40 MHz, $CDCl_3$) spectrum of the polymer drug conjugate (no. 8, Table 3).

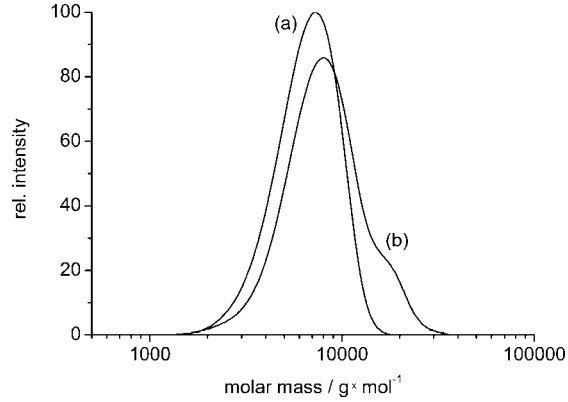


**Figure 14.** Gel permeation chromatographic profiles of (a) methylcoumarin end-functionalized poly(methyl methacrylate) (no. 7, Table 3) and (b) the corresponding polymer drug conjugate (no. 8, Table 3).

from typical methyl ester groups ($-OCH_3$) of PMMA at 3.51 ppm. A weak signal from the chain end methyl ester group ($-OCH_3$) of PMMA was observed at 3.58 ppm. We therefore calculated $M_n$ by $^1$H NMR spectroscopy from the resonance of the methyl ester groups ($-OCH_3$) of PMMA between 3.51 and 3.58 ppm and the C5H aromatic proton of coumarin functionality at 7.6 ppm. Polymerizations in anisole at 70 °C using an equimolar ratio of initiator to catalyst showed insufficient chain length control due to low initiator efficiencies ($f = M_{n,theor}/M_{n,measured}$; $M_{n,theor}$ = molar mass **A** + conversion/100 × molar mass MMA × [MMA]/[**A**]). Under comparable conditions, the copper-mediated ATRP of MMA displays a significantly higher equilibrium constant compared to styrene and methyl acrylate.[18] As a result of the increased concentration of growing radicals, chain termination and other side reactions occur more frequently. A good correlation of the theoretical molecular weight and the obtained molecular weight was therefore achieved when an initiator to catalyst ratio of 4:1 was used (Figure 6). The initiator

**Scheme 2. Photoinduced Drug Release by Single-Photon Absorption (SPA) and Subsequent Hydrolysis of the Pro-Drug 1-Heptanoyl-5-fluorouracil to 5-Fluorouracil**

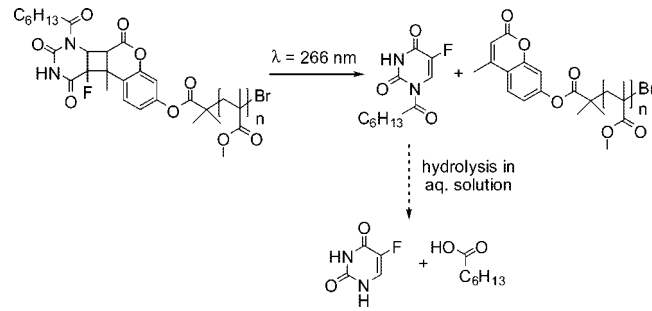


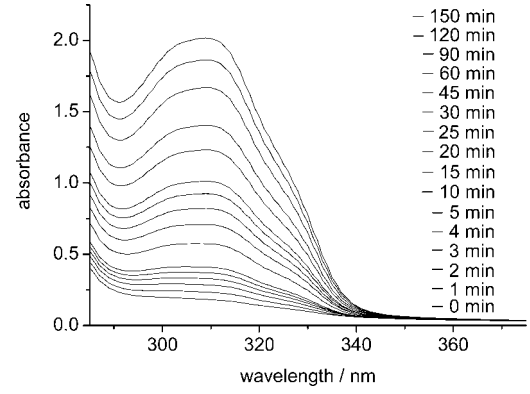


**Figure 15.** Time-dependent UV/vis absorption spectra of polymer drug conjugate (no. 8, Table 3; $c$ = 2.9 g/L in THF) during UV-light irradiation ($\lambda$ = 266 nm).

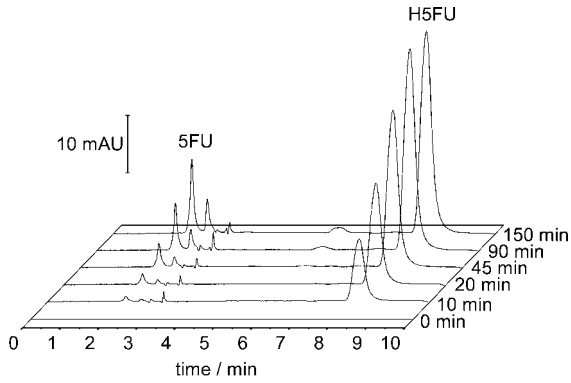


**Figure 16.** Time-dependent high-performance liquid chromatographic (HPLC) analysis of released compounds during UV irradiation ($\lambda$ = 266 nm). Solution of polymer drug conjugate (no. 8, Table 3) in THF ($c$ = 2.9 g/L). Cytostatic drug 5-fluorouracil (5FU) and pro-drug 1-heptanoyl-5-fluorouracil (H5FU) are marked.

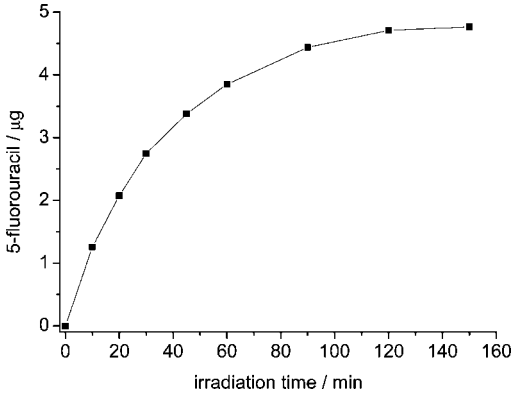


**Figure 17.** Recovery of 5-fluorouracil (quantitative hydrolysis of 1-heptanoyl-5-fluorouracil to 5-fluorouracil assumed; calculated for 1 mg of polymer drug conjugate) after exposure of a polymer solution (no. 8, Table 3, $c$ = 2.9 g/L in THF) to UV light ($\lambda$ = 266 nm).

efficiency increased from 0.57 to 0.78 (calculated from data in Table 1), while the polydispersity decreased to a minimum of $M_w/M_n$ = 1.13. Table 1 shows that the conversion decreased considerably on increasing the initiator to catalyst ratio, which is consistent with various kinetic studies that indicate the rate of a typical ATRP is first order with respect to monomer, initiator, and copper(I) complex concentrations.[19,20]

Further evidence that the polymer chains were essentially initiated by 7-(2′-bromoisobutyryloxy)-4-methylcoumarin (**A**) derives from the comparison of the GPC chromatograms recorded using refractive index and UV (264 nm) detectors (Figure 7). In case of methylcoumarin end-functionalized PMMA, a UV signal is expected while pure PMMA shows no detectable absorption at 264 nm.

The linear time dependence of $\ln([M]_0/[M])$ (Figure 8) is consistent with a controlled polymerization process that is first order in monomer concentration. Furthermore, the progression of molecular weight (Figure 9) is consistent with the kinetic model for a controlled polymerization process with a constant number of growing chains.

The effect of lowering the monomer to initiator feed ratio on molecular weight and monomer conversion was systematically studied, and the results are summarized in Table 1. GPC analysis confirms a good chain length control and an essentially controlled polymerization process when short oligomeric chains were targeted even at high conversion (Figure 10).

**Photochemical Drug Loading.** Photochemical drug loading of **B** was performed in solution (chloroform/acetone 1:2) with benzophenone as additional photosensitizer using a Rayonet-type photoreactor as described in the Experimental Section. To prevent polymer chains from undergoing the favored chain dimerization instead of drug loading, a 50-fold excess of the pro-drug 1-heptanoyl-5-fluorouracil (H5FU), **3**, was employed. Relatively long polymer chains ($M_n$ = 6020) were selected for the first drug loading experiments because in this case purification by precipitation after drug loading was straightforward whereas purification of oligomeric polymer drug conjugates **C** proved to be much more intricate and is currently under investigation.

The spectral properties of the polymer drug conjugate **C** and base polymer **B** are shown in Figure 11. The decrease of the absorption band at $\lambda \approx 270$ nm ($\pi \rightarrow \pi^*$ transition in coumarin and uracil derivatives)[21,22] is consistent with the photodimerization reaction and especially the leveling of the characteristic absorption maximum at $\lambda$ = 310 nm ($\pi \rightarrow \pi^*$ transition in the coumarin chromophore)[21] after UVA irradiation indicates almost quantitative reaction of the conjugated lactone double bond in a [2 + 2]-cycloaddition reaction (Scheme 1).

**C** was further analyzed by $^1$H and $^{19}$F NMR spectroscopy. The distinct differences between the $^1$H NMR spectra of the base polymer **B** and that of the polymer drug conjugate **C** are the absence of the olefinic proton resonance (Figure 12) at 6.23 ppm and the disappearance of the $C11H_3$ resonance signal at 2.40 ppm of the coumarin functionality, indicating the complete conversion of coumarin moieties into photodimers. Further proof for the formation of cyclobutane-type linkages to H5FU arises from the characteristic cyclobutane proton signals (C6′H and C3′H) at 5.16 and 5.09 ppm.

Use of $^{19}$F NMR spectroscopy permits not only verification of successful coumarin-H5FU cross-dimerization but also distinction between isomeric photodimers. The sole resonance signal at −138.1 ppm (Figure 13) suggests the exclusive formation of one of four possible isomers.

The change of polymer properties like thermal stability, glass transition, and molecular weight after photochemical drug immobilization was also of interest (Table 3). As expected, the glass transition temperature increased only negligibly for the H5FU-loaded polymer (Table 3). Unlike coumarin multifunctionalized copolymers,[13–16] no extensive photoinduced cross-linking reduced the polymer chain mobility. However, the thermal stability of the polymer drug conjugate (no. 8, Table 3) was considerably reduced compared to the corresponding base polymer (no. 7, Table 3) but was still sufficiently high enough for various molding techniques normally utilized for polymer processing. GPC analysis showed no detectable chain degradation due to UV irradiation. The GPC profiles indicated a bimodal molecular weight distribution which may be due to partial chain dimerization reactions during photochemistry (Figure 14), leading to the formation of some polymer−polymer conjugate besides the desirable polymer−drug conjugate.

**Photoinduced Drug Release by Single-Photon Absorption (SPA).** The characterization of the photoinduced drug release was investigated for a single-photon absorption (SPA) process. The polymer drug conjugate (No. 8, Table 3) was dissolved in THF and irradiated at $\lambda$ = 266 nm to cleave the cyclobutane linker between the methylcoumarin moiety and the pro-drug H5FU. In contrast to long wavelength UV irradiation ($\lambda$ > 300 nm), which promotes [2 + 2]-cycloaddition, the [2 + 2]-cycloreversion reaction predominates if using shorter wavelengths ($\lambda$ < 300 nm) (Scheme 2).

Since the absorption band at $\lambda$ = 310 nm is characteristic of the coumarin chromophore, it was monitored at different intervals of time during the drug release experiments. The strong increase of absorbance in this wavelength region indicates the re-formation of the coumarin double bond equivalent to photoinduced cleavage of cyclobutane linker groups of the polymer drug conjugate (Figure 15).

HPLC analysis finally allowed identification and quantification of any released compounds during irradiation. The chromatograms (Figure 16) display the time-dependent accumulation of free H5FU and 5FU in the polymer solution. The elution times of H5FU and 5FU were established using the corresponding standards. The origin of the other signals is not known at this time and currently under investigation, but it is likely that photoinduced degradation is responsible for those impurities. The hydrolysis of H5FU to 5FU has been reported to be quantitative within 20 h.[16] Assuming quantitative hydrolysis, 4.76 $\mu$g of 5FU per 1 mg of polymer drug conjugate (No. 8, Table 3) was released after an irradiation time of 150 min (Figure 17). The LD50 (lethal dose at which 50% of subjects will die) of 5-fluorouracil, which was reported for rabbit lens epithelial cells (RLEC) to be 0.58 $\mu$g/mL,[23] can easily be realized even with small weight fractions of polymer drug conjugate blended with a high molecular weight polyacrylate matrix used as lens precursor.

## Conclusions

The successful synthesis of novel coumarin end-functionalized poly(methyl methacrylate) polymers of different molecular weights by atom transfer radical polymerization were realized. By reducing the functionalization to one coumarin linker-unit per polymer chain, we avoided intramolecular cross-linking and limited intermolecular cross-linking to chain dimerization during the photochemical drug loading process and hence provided an advantage over the previous multifunctional approach to the problem. Photoinduced drug release using single-photon absorption (SPA) was also shown to work for this system. The quantification of the drug released on single-photon absorption showed the realization of LD50 of 5-fluorouracil with even very small amounts of polymer drug conjugate. Presently, the system is being tested for drug release studies using two-photon absorption (TPA). TPA will have no harmful effect on human tissues and also expected to reduce photodegradation products and will actually be used in clinical drug release process.

**Acknowledgment.** The authors are indebted to BMBF for financial support.

## References and Notes

(1) Uhrich, K. E.; Cannizzaro, S. M.; Langer, R. S.; Shakesheff, K. M. *Chem. Rev.* **1999**, *99*, 3181–3198.
(2) DeBoer, A. G.; Breimer, D. D. *J. R. College Phys. London* **1994**, *28*, 502–506.
(3) Domb, A. J. *Polymeric Site-Specific Pharmacotherapy*; John Wiley & Sons: Chicester, UK, 1994.
(4) Walter, K. A.; Tamargo, R.; Olivi, A.; Burger, P. C.; Brem, H. *Neurosurgery* **1995**, *37*, 1129–1145.
(5) Jantzen, G. M.; Robinson, J. R. *Modern Pharmaceutics*, 3rd ed.; Marcel Dekker: New York, 1996.
(6) Langer, R. *Science* **1990**, *249*, 1527–1533.
(7) Trinavarat, A.; Atchaneeyasakul, L.-o.; Udompunturak, S. *J. Cataract Refractive Surg.* **2001**, *27*, 775–780.
(8) Lee, J.-S.; Li, C.-Y.; Lin, Y.-C.; Chang, S.-Y.; Lin, K.-K. *J. Cataract Refractive Surg.* **2003**, *29*, 621–623.
(9) Ge, J.; Wand, M.; Chiang, R.; Paranhos, A.; Shields, B. *Arch. Ophthalmol.* **2000**, *118*, 1334–1337.
(10) Channell, M. M.; Beckman, H. *Arch. Ophthalmol.* **1984**, *102*, 1024–1026.
(11) Ranta, P.; Tommila, P.; Kivelä, T. *J. Cataract Refractive Surg.* **2004**, *30*, 58–66.
(12) Olsen, G.; Olson, R. J. *J. Cataract Refractive Surg.* **2000**, *26*, 1017–1021.
(13) Hampp, N.; Kim, H.-C.; Kreiling, S.; Hesse, L.; Greiner, A. *Proc. SPIE* **2003**, *5142*, 161–168.
(14) Kim, H.-C.; Härtner, S.; Behe, M.; Behr, T. M.; Hampp, N. *J. Biomed. Opt.* **2006**, *11*, 034024-1–034024-9.
(15) Kim, H.-C.; Härtner, S.; Hampp, N. *Proc. SPIE* **2006**, *6138*, 61380S-1–61380S-8.
(16) Kim, H.-C.; Kreiling, S.; Härtner, S.; Hesse, L.; Greiner, A.; Hampp, N. *Proc. SPIE* **2004**, *5323*, 327–334.
(17) Jolimaitre, P.; Andre-Barres, C.; Malet-Martino, M.; Martino, R.; Rico-Lattes, I. *Synlett* **1999**, *11*, 1829–1831.
(18) Matyjaszewski, K.; Xia, J. *Chem. Rev.* **2001**, *101*, 2921–2990.
(19) Percec, V.; Barboiu, B.; Kim, H.-J. *J. Am. Chem. Soc.* **1998**, *120*, 305–316.
(20) Wang, J.-L.; Grimaud, T.; Matyjaszewski, K. *Macromolecules* **1997**, *30*, 6507–6512.
(21) Seixas de Melo, J. S.; Becker, R. S.; Macanita, A. L. *J. Phys. Chem.* **1994**, *98*, 6054–6058.
(22) Gustavsson, T.; Bányász, Á.; Lazzarotto, E.; Markovitsi, D.; Scalmani, G.; Frisch, M. J.; Barone, V.; Improta, R. *J. Am. Chem. Soc.* **2006**, *128*, 607–619.
(23) Su, X.; Li, S.; Zheng, J. *Zhonghua Yan Ke Za Zhi* **1996**, *32*, 339–341.

MA702622P